



# Classifications of Qualitative Characteristics on Angle Configurations via Ultrasound Biomicroscopy in Acute Primary Angle Closure

Fenglei Wang , Dabo Wang, Ling Wang 

Department of Ophthalmology, the Affiliated Hospital of Qingdao University, Qingdao University, Qingdao, People's Republic of China

Correspondence: Ling Wang, Department of Ophthalmology, the Affiliated Hospital of Qingdao University, Qingdao University, No. 16 Jiangsu Road, Shinan District, Qingdao, 266003, People's Republic of China, Tel +86-18661806679, Email tsingtaowl@hotmail.com

**Purpose:** To study the classifications of qualitative characteristics on the angle configurations in the acute primary angle closure (APAC) and fellow eyes by ultrasound biomicroscopy (UBM).

**Methods:** A total of 131 patients (262 eyes) were researched retrospectively. The qualitative parameters from UBM images were classified into iris form (IF), ciliary body configuration (CBC), basal iris thickness (BIT), iris convexity (IC), iris insert (II), iris angulation (IA), ciliary body size (CBS) and ciliary body position (CBP). Comparative analyses between the APAC (case group) and fellow (control group) eyes were performed.

**Results:** There were significant differences in IF, CBC, IC, II, CBS, CBP between the case group and control group in all quadrants ( $P<0.001$ ). The IA of the case group and control group presented significant difference in all quadrants ( $P=0.001$ ). However, there was not a significant difference in BIT between the case group and control group in all quadrants ( $P=0.495$ ). The case group had fewer parallelogram-like and mushroom-like and more cone-like and hook-like CBCs than the control group ( $P<0.001$ ).

**Conclusion:** Multiple ciliary body configurations can influence the stability of the lens and the anatomic configuration of the anterior chamber angle indirectly. New qualitative classification system of UBM may be more intuitionistic and refined to reflect the angle configurations to help clinical practice.

**Keywords:** acute primary angle closure, qualitative parameter, angle configuration, ultrasound biomicroscopy

## Introduction

Population-based epidemiological surveys have shown that the incidence of angle-closure glaucoma (ACG) is higher in the East Asian population than in European and African populations.<sup>1</sup> Of ACG patients, 87% live in Asia. In 2010, 280,000 people lost their vision due to glaucoma in East Asia.<sup>2,3</sup> Two million Chinese people have blindness in at least one eye due to primary angle-closure glaucoma (PACG), and it is expected that PACG will be the cause of nearly half of all cases of binocular blindness in 2020.<sup>1,3,4</sup>

Acute primary angle closure (APAC) can cause an acute decline in vision within a short period and irreversibly damage the optic nerve; patients' quality of vision can be seriously affected.<sup>5</sup> With the widespread application of imaging technology in ophthalmology, we have a more in-depth understanding of the pathogenesis of APAC, but there is no consensus on the mechanism of angle closure. In patients with APAC, both eyes have the similar anatomical structures, but why is it that only one eye experiences the acute attack? Which anatomical features of the affected eye are related to the occurrence of acute angle-closure? Some well-known mechanisms include the pupillary block mechanism, non-pupillary block mechanism, and the combination of multiple mechanisms.<sup>6</sup> APAC is more likely to occur in crowded anterior chambers, and previous studies have reported that short axial length, narrow drainage angle, shallow anterior chamber, and a more anterior lens position are major anatomical factors that can lead to its occurrence.<sup>7</sup> Some studies

have shown that a greater iris convexity and a more anterior insertion of the iris root also facilitate APAC.<sup>6</sup> Other studies have also examined the contribution of dynamic factors such as choroidal expansion to APAC.<sup>8</sup>

Ultrasound biomicroscopy (UBM), a non-invasive high-resolution in vivo anterior imaging technique, has proven to be highly advantageous in assessing the structure of the anterior chamber angle.<sup>9</sup> UBM provides a means for imaging and assessing morphological structures of the anterior segment of the eye (including the ciliary body, zonular apparatus and its attachment to the equatorial region of the lens which cannot be seen on routine slit lamp exam). In addition, UBM can be used to perform quantitative and qualitative analyses of pathophysiologic changes in the structures of the anterior segment.<sup>10,11</sup> In studies on angle-closure (AC) diseases, the geometric angle quantification software included in ultrasound biomicroscopes can be utilised to indicate the iris thickness, ciliary body size and the anatomical and positional relationships between the iris and ciliary body. Due to the advantages of ultrasound biomicroscopy (UBM) in diagnosing APAC, it was used to assess the relevant parameters in this study.

In this study, we established a new qualitative assessment system, by which qualitative data (including CBC and IF) acquired from UBM images of APAC and fellow eyes were comparatively analysed for the first time. Through the comparison of the anatomical differences in angle configuration, we investigated the diverse factors involved in the occurrence mechanisms of APAC.

## Materials and Methods

### Materials

#### Study Population

131 patients (262 eyes) with monocular APAC who were hospitalised for treatment at the Affiliated Hospital of Qingdao University between October 2013 and October 2018 were recruited into the study. The participants consisted of 110 women (220 eyes, 83.97%) and 21 men (42 eyes, 16.03%) with a mean age of  $66.09 \pm 8.52$  years. (Table 1)

A written informed consent form was signed by each subject. All procedures of this study were conducted in compliance with the Declaration of Helsinki.

#### Inclusion and Exclusion Criteria<sup>12</sup>

1. No major underlying disease requiring medical or surgical intervention and a history of ocular trauma.
2. Unilateral acute angle-closure glaucoma, with the time of onset less than 5 days. Before admission, neither of the eyes has received medication, laser or surgical intervention (including anterior chamber puncture treatment).
3. No any ophthalmic diseases affecting the chamber angle.
4. Typical characteristics of acute angle-closure crisis (AACC).<sup>5,13</sup>
5. Excluding patients with allergy to the mydriatic agent (Eye drops containing 0.5% tropicamide and 0.5% phenylephrine hydrochloride) and surface anesthetic agent (0.4% oxybuprocaine solution, 20mL:80mg).
6. Excluding patients with poor image clarity in UBM, A-Scan and other imaging examinations.
7. Excluding patients with incomplete clinical data.

**Table 1** Baseline Demographics and Clinical Data of Research Participants

Variable	APAC (131)	Fellow (131)	P
Sex (F/M) n	110/21	110/21	
Sex (F/M)%	83.97/16.03	83.97/16.03	
Age <sup>a</sup> (years)	66.09±8.52	66.09±8.52	
OD/OS	65/66	66/65	0.823
Attack time <sup>a</sup> (days)	2.45±2.29		
IOP <sup>a</sup> (mm Hg)	35.31±15.99	16.23±3.98	<0.001
BCVA <sup>a</sup> (Decimal)	0.21±0.26	0.66±0.30	<0.001
Sphere <sup>a</sup> (Diopter)	0.84±2.06	0.81±2.01	0.857
Cylinder <sup>a</sup> (Diopter)	-0.17±1.12	-0.18±1.08	0.976

Note: <sup>a</sup>Continuous variables are expressed as mean ± SD.

Abbreviations: F, female; M, male; OD, right eye; OS, left eye; IOP, intra-ocular pressure; BCVA, best corrected visual acuity.

## Methods

### Routine Ophthalmic Examination

All participants underwent a detailed ophthalmic examination including autorefraction (Topcon Ltd, KR-8900, Japan), best corrected visual acuity (Topcon Ltd, CV-5000, Japan), intraocular pressure (IOP) (Goldmann applanation tonometer), slit lamp (Haag-Streit Ltd, BM 900, Switzerland), fundus examination (Volk Ltd, VSFNC, USA) and gonioscopy (Ocular Ltd, OSMG, USA).

UBM (SW3200L, Suoer, China) was used to display qualitative parameters of anterior chamber angle.<sup>14,15</sup> A 50MHz transducer was used to measure each local image at 3:00, 6:00, 9:00 and 12:00, and panoramic image at 12:00–6:00 and 3:00–9:00 respectively in the darkroom with 60–70LUX of light illumination and in a supine position under topical anesthesia. UBM was performed by two experienced ophthalmic technicians. The ideal image could clearly reveal the scleral process and ciliary body configuration and iris form, and the long axis of the lens was located in the horizontal position with showing the front surface of the lens precisely. Manual labeling and analysis of UBM images were performed by two experienced ophthalmic glaucoma clinicians. Each image was respectively analyzed by two doctors (randomized and masked), and immediately outputted by joint evaluation.<sup>12</sup>

### Classifications and Types of Qualitative Parameters<sup>16</sup>

The morphological features revealed on UBM were allocated to eight main classifications (Figure 1): iris form (IF), ciliary body configuration (CBC), basal iris thickness (BIT), iris convexity (IC), iris insert (II), iris angulation (IA), ciliary body size (CBS), and ciliary body position (CBP).

IF was classified into five types (Figure 1A):

Type 1 - Forward bowing of the entire iris

Type 2 - Backward bowing of the entire iris

Type 3 - Flat iris

Type 4 - Forward bowing of the central iris with backward bowing of the basal iris

Type 5 - Forward bowing of the basal iris with backward bowing of the central iris

CBC was classified into 4 types (Figure 1B):

Type 1 - Parallelogram-like

Type 2 - Cone-like

Type 3 - Mushroom-like

Type 4 - Hook-like

The CBC was defined as the general configuration of the ciliary body along its long axis, regardless of the shape of the pars plana. It is the shape enclosed by the yellow lines.

BIT was classified into three types (Figure 1C):

Type 1 -  $BIT < 1/2$  corneal limbus thickness (CLT)

Type 2 -  $BIT = 1/2$  CLT

Type 3 -  $BIT > 1/2$  CLT

The BIT was defined as the vertical thickness at the peripheral 1/3 of the iris (marked by the yellow line on iris). This can represent the average thickness of the entire iris. The CLT (marked by the short yellow line on the sclera) was measured as the line perpendicular to the line connecting the sclera spur to the outer edge of the sclera (marked by the long yellow line on the sclera). The 1/2 of CLT is marked by the red line.

IC was classified into four types (Figure 1D):

Type 1 - Posterior bowing of iris ( $IC < 0$  mm) or flat iris ( $IC = 0$  mm)

Type 2 - Mild anterior bowing of iris ( $0 \text{ mm} < IC \leq 0.2 \text{ mm}$ )

Type 3 - Moderate anterior bowing of iris ( $0.2 \text{ mm} < IC \leq 0.4 \text{ mm}$ )

Type 4 - Severe anterior bowing of iris ( $IC > 0.4 \text{ mm}$ )

IC was defined as the curvature of the back surface of iris measured by the red line perpendicular between the yellow line connecting the most central part of iris to iris root and the iris vault.<sup>16–20</sup> With the values of IC measured in the second part, the degree of iris bombe can be classified precisely.

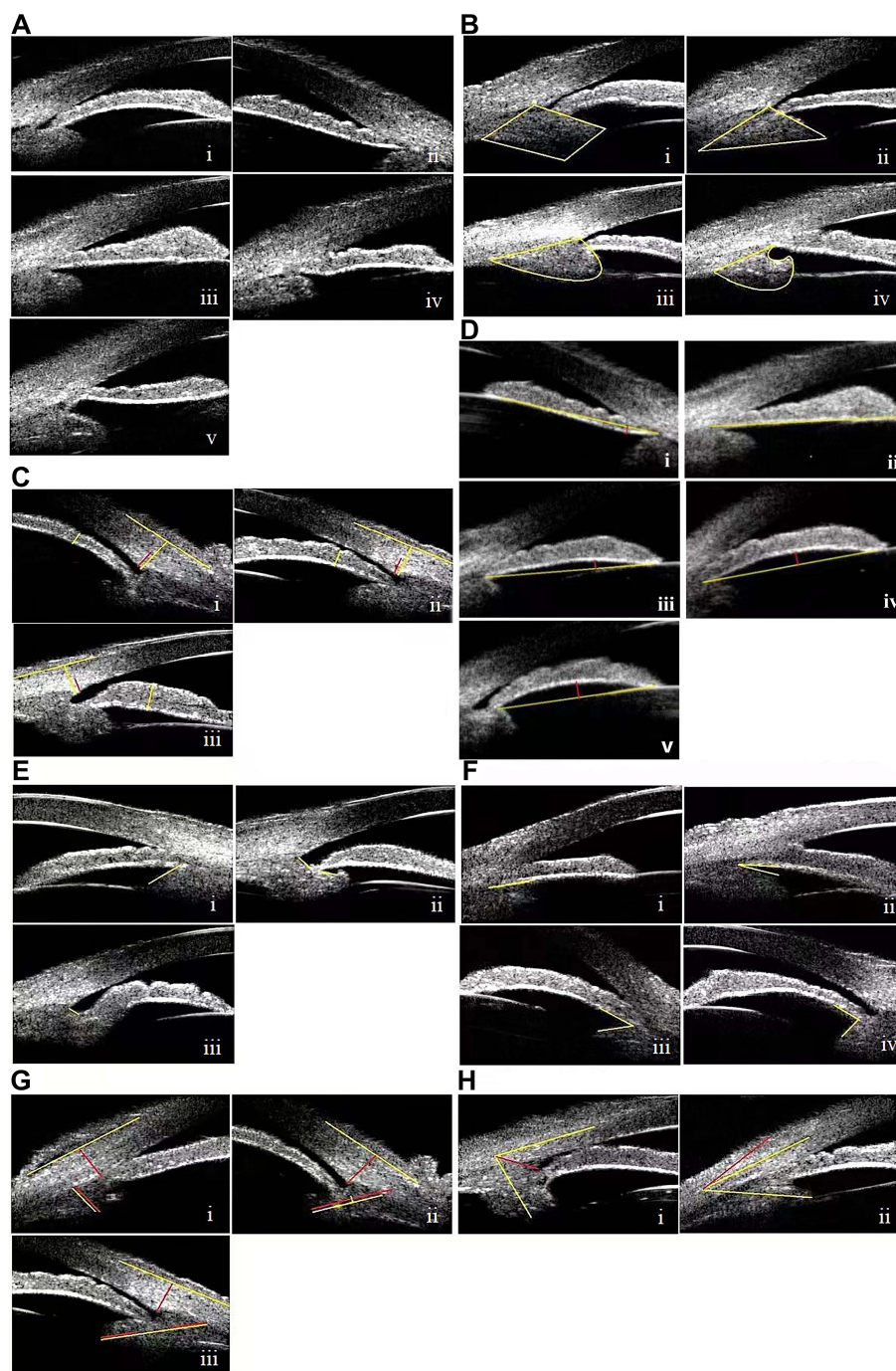


**Figure 1** Morphological classifications and types of qualitative parameters revealed on UBM images (A–H). (A) Iris Form (IF) included 5 types, forward bowing of the entire iris (Ai); backward bowing of the entire iris (Aii); flat iris (Aiii); forward bowing of the central iris with backward bowing of the basal iris (Aiv); forward bowing of the basal iris with backward bowing of the central iris (Av). (B) Ciliary body configuration (CBC) included 4 types, parallelogram-like (Bi); cone-like (Bii); mushroom-like (Biii); hook-like (Biv). CBC is a shape surrounded by yellow lines. (C) Basal iris thickness (BIT) included 3 types,  $< 1/2$  corneal limbus thickness (CLT) (Ci);  $= 1/2$  CLT (Cii);  $> 1/2$  CLT (Ciii). The yellow line on iris means the vertical thickness at the peripheral  $1/3$  of the iris. The short and long yellow lines on the sclera mean the CLT and outer edge of the sclera. The  $1/2$  of CLT is marked by the red line. (D) Iris convexity (IC) included 4 types, posterior bowing of iris ( $IC < 0$  mm) (Di) or flat iris ( $IC = 0$  mm) (Dii); mild anterior bowing of iris ( $0 \text{ mm} < IC \leq 0.2$  mm) (Diii); moderate anterior bowing of iris ( $0.2 \text{ mm} < IC \leq 0.4$  mm) (Div); severe anterior bowing of iris ( $IC > 0.4$  mm) (Dv). The yellow line connects the most central part of iris to iris root. The red line is perpendicular between the yellow line and the iris vault. (E) Iris insert (II) included 3 types, base of the ciliary body (Ei); middle part of the ciliary body (Eii); apex of the ciliary body (Eiii). The yellow line shows the remaining position of the anterior surface of the ciliary body after iris insert. (F) Iris angulation (IA) included 4 types,  $IA = 0^\circ$  (Fi);  $0^\circ < IA \leq 30^\circ$  (Fii);  $30^\circ < IA \leq 60^\circ$  (Fiii);  $IA > 60^\circ$  (Fiv). The two yellow lines mean the back surface of the iris and the anterior surface of the ciliary processes. (G) Ciliary body size (CBZ) included 3 types,  $CBS \leq 1$  CLT (Gi);  $1 \text{ CLT} < CBS \leq 2 \text{ CLT}$  (Gii);  $CBS > 2 \text{ CLT}$  (Giii). The yellow line on the ciliary body connects the midpoint of the ciliary processes to the center of the base of the ciliary body. The red line on the sclera means the corneal limbus thickness. (H) Ciliary body position (CBP) included 2 types, Backward rotation  $\geq 45^\circ$  (Hi); Forward rotation  $< 45^\circ$  (Hii). The yellow line on the limbus connects the midpoint of the CLT to the midpoint of the thickness at the mid-peripheral  $1/3$  of the cornea. The yellow line on the ciliary body connects the midpoint of the ciliary processes to the center of the base of the ciliary body. The angle between the red line and the yellow line on the ciliary body is  $45^\circ$ .

II was classified into three types (Figure 1E):

- Type 1 - Base of the ciliary body (scleral spur)
- Type 2 - Middle part of the ciliary body
- Type 3 - Apex of the ciliary body

II was classified according to the location of the iris root insertion and attachment. Type 1 means that the iris root is attached to the scleral spur, accompanied by trabecular-iris contact, and the disappearance of the anterior chamber angle. Type 2 and 3 mean that the iris roots are attached to the middle part and apex of the ciliary body with angle open.

IA was classified into four types (Figure 1F):

- Type 1 -  $IA = 0^\circ$
- Type 2 -  $0^\circ < IA \leq 30^\circ$
- Type 3 -  $30^\circ < IA \leq 60^\circ$
- Type 4 -  $IA > 60^\circ$

IA was classified according to the angle of the insertion of the iris root into the ciliary body. IA (the angle marked by the yellow lines) is defined as the angle formed between the back surface of the iris and the anterior surface of the ciliary processes, which can reflect the spatial relation between the ciliary processes and the iris root.

CBS was classified into three types (Figure 1G):

- Type 1 -  $CBS \leq 1 \text{ CLT}$
- Type 2 -  $1 \text{ CLT} < CBS \leq 2 \text{ CLT}$
- Type 3 -  $CBS > 2 \text{ CLT}$

CBS (marked by the yellow line on the ciliary body) was defined as the length of the line connecting the midpoint of the ciliary processes to the center of the base of the ciliary body, which represents the average length of the ciliary body. The CLT (marked by the red line on the sclera) was defined as the line perpendicular to the line connecting the sclera spur to the outer edge of the sclera (marked by the yellow line on the sclera).

CBP was classified into two types (Figure 1H):

- Type 1 - Backward rotation  $\geq 45^\circ$
- Type 2 - Forward rotation  $< 45^\circ$

CBP was defined as the angle formed by the extension of two lines; one connecting the midpoint of the ciliary processes to the center of the base of the ciliary body (marked by the yellow line on the ciliary body) and the other connecting the midpoint of the CLT (found using the aforementioned method) to the midpoint of the thickness at the mid-peripheral 1/3 of the cornea (marked by the yellow line on the limbus). CBP directly reflects the spatial relation between the ciliary body and the limbus (forward or backward rotation). The angle between the red line and the yellow line on the ciliary body is  $45^\circ$ .

## Statistical Analysis

SPSS 20.0 statistical software was used for data analysis. The paired *t*-test was used to compare and analyze the demographic characteristics and clinical data of the case and the control groups (the data conformed to the normal distribution). The paired chi-squared test was used to compare the differences in the qualitative data of the eye with APAC and the contralateral eye shown by UBM images. The Pearson chi-square value was calculated. A multivariate histogram of the differences in the qualitative data obtained from the UBM images was drawn.  $P < 0.05$  indicated statistical significance.

## Results

### Demographic Characteristics and Clinical Data

Table 1 shows the baseline demographic composition and clinical data of the case and control groups. The duration of an episode in the case group was  $2.45 \pm 2.29$  days. The IOP was significantly higher in the case group ( $35.31 \pm 15.99$  mmHg) than in the control group ( $16.23 \pm 3.98$  mmHg) ( $P < 0.001$ ). The best-corrected visual acuity was significantly lower in the case group ( $0.21 \pm 0.26$ ) than in the control group ( $0.66 \pm 0.30$ ) ( $P < 0.001$ ). There was no significant difference in the spherical and cylindrical refractive errors between the case and control groups. ( $P > 0.05$ ).



## Chi-Square Analysis

Table 2 showed the comparison between the qualitative data for all quadrants of the case and control groups.

There was a significant difference between the IFs of the case and control groups ( $\chi^2 = 108.446$ ;  $P < 0.001$ ). The proportion of forward bowing was lower in the case group than in the control group, while the proportions of the flat iris, backward bowing, forward bowing of the central iris with backward bowing of the basal iris, and forward bowing of the basal iris with backward bowing of the central iris were higher in the case group than in the control group. There were significant differences between the CBCs of all the quadrants in the case and control groups ( $\chi^2 = 53.890$ ;  $P < 0.001$ ). The case group had fewer parallelogram-like and mushroom-like and more cone-like and hook-like CBCs than the control group. There was no significant difference between the BICs of all quadrants in the case and control groups ( $\chi^2 = 1.407$ ;  $P = 0.495$ ). There

**Table 2** Morphological Classifications and Types of Qualitative Parameters in APAC and Fellow Eyes

n (%)	APAC	All Quadrants		$\chi^2$
		Fellow	P	
IF				
Type 1	401(76.41)	503(95.94)	<0.001	108.446
Type 2	12(2.34)	2(0.47)		
Type 3	17(3.28)	8(1.56)		
Type 4	76(14.53)	11(2.03)		
Type 5	18(3.44)	0(0.00)		
CBC				
Type 1	161(30.78)	230(43.91)	<0.001	53.890
Type 2	180(34.38)	98(18.75)		
Type 3	65(12.34)	97(18.44)		
Type 4	118(22.50)	99(18.90)		
BIT				
Type 1	50(9.53)	42(7.97)	0.495	1.407
Type 2	283(54.06)	297(56.72)		
Type 3	191(36.41)	185(35.31)		
IC				
Type 1	103(19.69)	20(3.75)	<0.001	182.738
Type 2	252(48.12)	153(29.22)		
Type 3	131(25.00)	239(45.62)		
Type 4	38(7.19)	112(21.41)		
II				
Type 1	449(85.78)	169(32.19)	<0.001	379.960
Type 2	69(13.13)	331(63.12)		
Type 3	6(1.09)	24(4.69)		
IA				
Type 1	43(8.28)	48(9.22)	0.001	16.587
Type 2	142(27.04)	96(18.28)		
Type 3	215(41.09)	221(42.19)		
Type 4	124(23.59)	159(30.31)		
CBS				
Type 1	56(10.62)	12(2.35)	<0.001	59.288
Type 2	404(77.19)	386(73.59)		
Type 3	64(12.19)	126(24.06)		
CBP				
Type 1	258(49.22)	329(62.81)	<0.001	24.001
Type 2	266(50.78)	195(37.19)		

**Note:** Categorical variables are expressed as frequency (%).

**Abbreviations:** APAC, acute primary angle closure; IF, iris form; CBC, ciliary body configuration; BIT, basal iris thickness; IC, iris convexity; II, iris insert; IA, iris angulation; CBS, ciliary body size; CBP, ciliary body position.

were significant differences between the ICs of all quadrants in the case and control groups ( $\chi^2 = 182.738$ ;  $P < 0.001$ ). The case group had more type 1 and type 2 and fewer type 3 and type 4 ICs than the control group. There were significant differences between the IIs of all quadrants in the case and control groups ( $\chi^2 = 379.960$ ;  $P < 0.001$ ). The case group had more type 1 and fewer type 2 and type 3 IIs than the control group. There were significant differences between the IAs of all quadrants in the case and control groups ( $\chi^2 = 16.587$ ;  $P = 0.001$ ). The case group had more type 1, type 3, and type 4 and fewer type 2 IAs than the control group. There were significant differences between the CBSs of all quadrants in the case and control groups ( $\chi^2 = 59.288$ ;  $P < 0.001$ ). The case group had more type 1 and type 2 and fewer type 3 CBSs than the control group. There were significant differences in the CBPs of all quadrants in the case and control groups ( $\chi^2 = 24.001$ ;  $P < 0.001$ ). The case group had fewer type 1 (backward rotation) and more type 2 (forward rotation) CBPs than the control group.

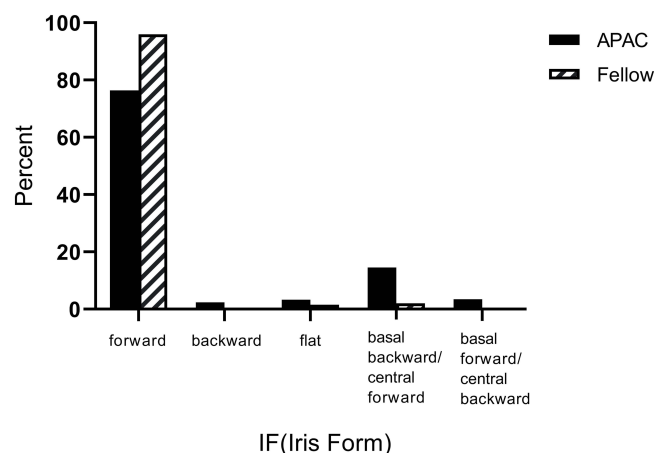
## Histograms

Figure 2 showed that in the case group, the proportions of type 1 IF (forward bowing of the entire iris), type 4 IF (forward bowing of the central iris with backward bowing of the basal iris), type 5 IF (forward bowing of the basal iris with backward bowing of the central iris), type 3 IF (flat iris), and type 2 IF (backward bowing of the entire iris) decreased sequentially. In the control group, the proportions of type 1 IF (forward bowing of the entire iris), type 4 IF (forward bowing of the central iris with backward bowing of the basal iris), type 3 IF (flat iris), type 2 IF (backward bowing of the entire iris), and type 5 IF (forward bowing of the basal iris with backward bowing of the central iris) decreased sequentially. Most of the IFs of the case and the control groups were type 1. The proportion of type 1 IF was significantly higher in the control group than in the case group, while the proportion of the other four types of IF was significantly higher in the case group than in the control group ( $\chi^2 = 108.446$ ;  $P < 0.001$ ).

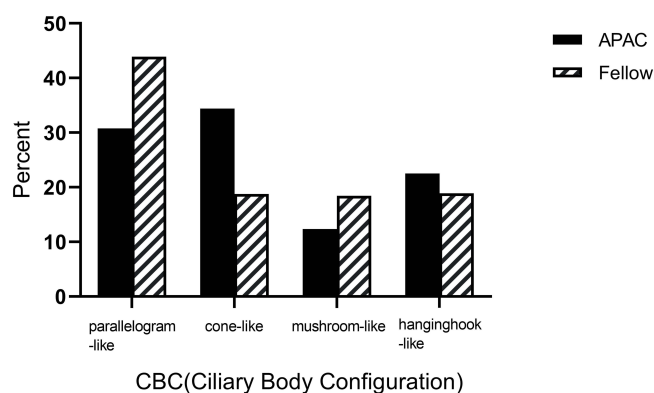
Figure 3 showed that in the case group, the proportions of cone-like CBC (type 2), parallelogram-like CBC (type 1), hook-like CBC (type 4), and mushroom-like CBC (type 3) decreased sequentially. In the control group, the dominant type was the parallelogram-like CBC (type 1), and the proportions of the other three types were generally the same. The proportions of type 2 and type 4 CBCs were significantly higher in the case group than in the control group, while the proportions of type 1 and type 3 CBCs were significantly higher in the control group than in the case group ( $\chi^2 = 53.890$ ;  $P < 0.001$ ).

Figure 4 showed that there were no significant differences between the proportions of the BIT types in the case and control groups ( $\chi^2 = 1.407$ ;  $P = 0.495$ ).

Figure 5 showed that the proportions of type 2 IC, type 3 IC, type 1 IC, and type 4 IC in the case group decreased sequentially, and the proportions of type 3 IC, type 2 IC, type 4 IC, and type 1 IC in the control group decreased sequentially. The case group had more type 2 ICs, while the control group had more type 3 ICs. The proportions of type 1 and type 2 ICs were significantly higher in the case group than in the control group, while the proportions of type 3 and type 4 ICs were significantly higher in the control group than in the case group ( $\chi^2 = 182.738$ ;  $P < 0.001$ ).



**Figure 2** Comparisons on the percentage of IF types between APAC and fellow eyes.



**Figure 3** Comparisons on the percentage of CBC types between APAC and fellow eyes.

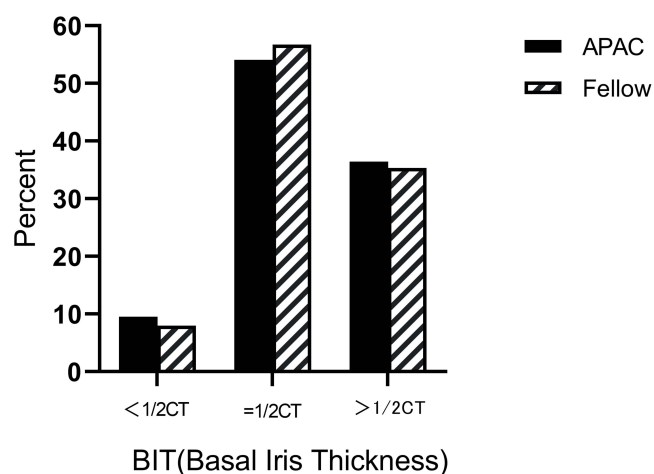


**Figure 4** Comparisons on the percentage of BIT types between APAC and fellow eyes.

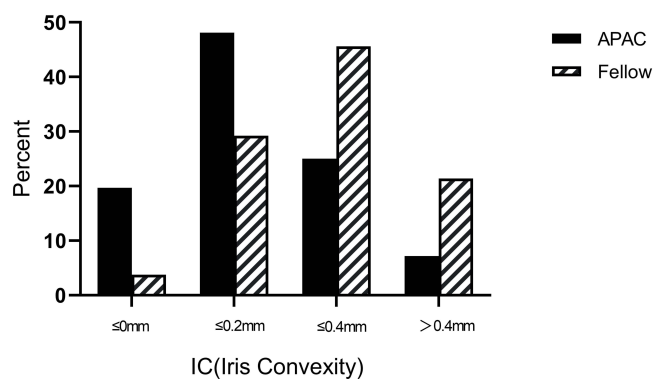


**Figure 5** Comparisons on the percentage of IC types between APAC and fellow eyes.

Figure 6 showed that the proportions of IIs at the base (type 1), the middle part (type 2), and the apex (type 3) decreased sequentially in the case group, while the proportions of II at the middle part (type 2), the base (type 1), and the apex (type 3) decreased sequentially in the control group. The case group had more type 1 IIs, while the control group had more type 2 IIs. The proportion of type 1 II was significantly higher in the case group than in the control group, and



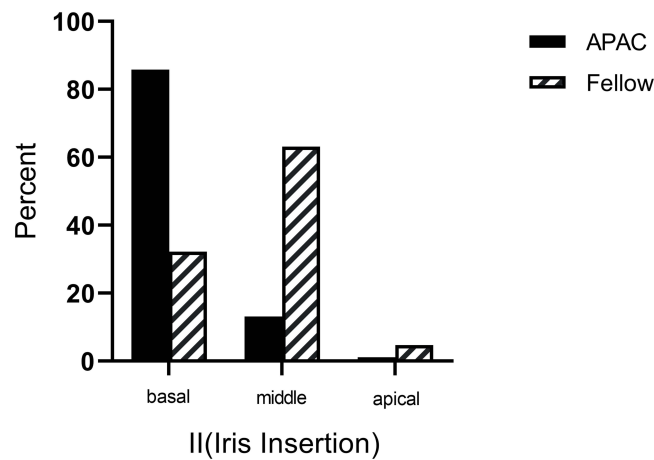


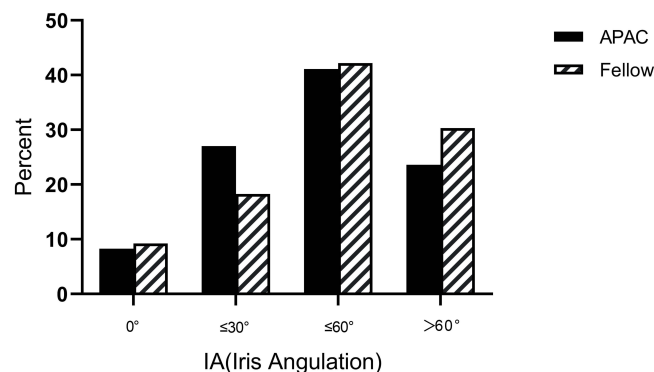
**Figure 6** Comparisons on the percentage of II types between APAC and fellow eyes.

the proportions of type 2 and type 3 IIs were significantly higher in the control groups than in the case group ( $\chi^2 = 379.960$ ;  $P < 0.001$ ).

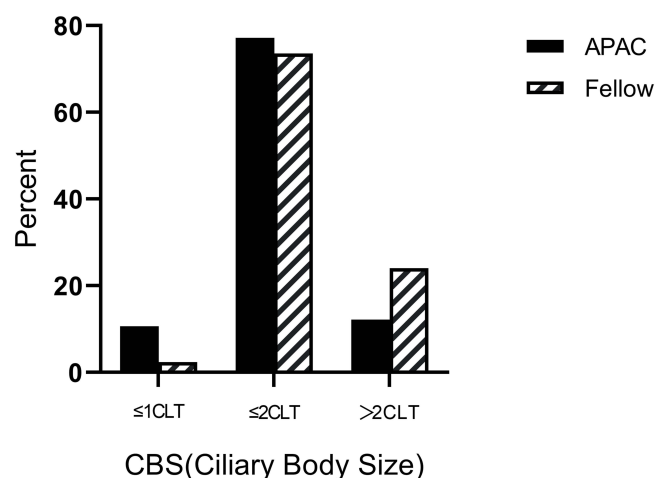
Figure 7 showed that the proportions of type 3, type 2, type 4, and type 1 IAs in the case group decreased sequentially, and the proportions of type 3, type 4, type 2, and type 1 IA in the control group decreased sequentially. Both groups had more type 3 IAs. The proportion of type 2 IA was significantly higher in the case group than in the control group, while the proportions of type 1, type 3, and type 4 IAs were significantly higher in the control group than in the case group ( $\chi^2 = 16.587$ ;  $P = 0.001$ ).

Figure 8 showed that the proportions of type 2, type 3, and type 1 CBSs decreased sequentially in both groups. Both groups also had more type 2 CBSs. The proportions of type 1 and type 2 CBSs were significantly higher in the case group than in the control group, and the proportion of type 3 CBS was significantly higher in the control group than in the case group ( $\chi^2 = 59.288$ ;  $P < 0.001$ ).

Figure 9 showed that the proportions of type 2 (forward rotation) and type 1 (backward rotation) CBPs decreased sequentially in the case group. In the control group, the proportions of type 1 and type 2 CBPs decreased sequentially. The proportion of type 2 CBP was significantly higher in the case group than in the control group, and the proportion of type 1 CBP was significantly higher in the control group than in the case group ( $\chi^2 = 24.001$ ;  $P < 0.001$ ).



**Figure 7** Comparisons on the percentage of IA types between APAC and fellow eyes.



**Figure 8** Comparisons on the percentage of CBS types between APAC and fellow eyes.

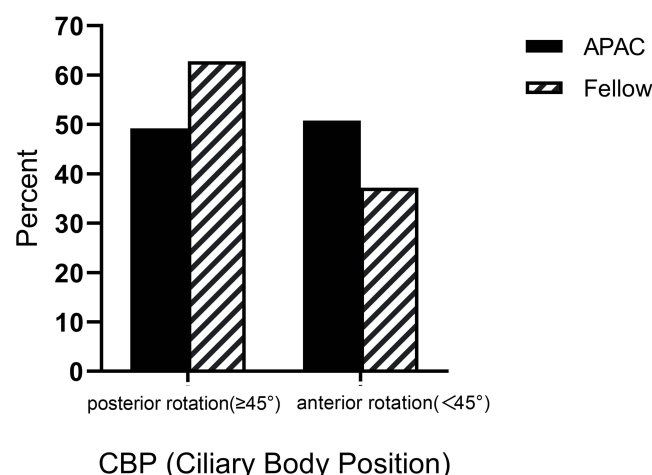


**Figure 9** Comparisons on the percentage of CBP types between APAC and fellow eyes.

## Discussion

In this study, a comprehensive morphological classification of the configurations of the angles on the UBM images of APAC eyes and fellow eyes was performed. The various qualitative indicators showed the morphological structures and spatial locations of the iris and ciliary body. This study is an extension of our previous series of related studies.<sup>12,21</sup> Compared with the classification standard in the Liwan eye study,<sup>16</sup> we included the IF and the CBC, which were additions that intuitively represented the morphological features of the iris and ciliary body and indirectly reflected their mechanical characteristics. The qualitative parameters IA, CBP, and IC also corresponded to the quantitative parameters ICPA, LCBA, and IC that we examined in our previous study.<sup>12</sup> The classification and comparative analysis of the configurations of the angles can help us to comprehensively analyze the characteristics of eyes with APAC.

In this study, we found that the case and control groups had more type 1 IF (forward bowing of the entire iris type). The proportion of type 1 IF was significantly higher in the control group than in the case group, while the proportions of the other four types of IF were significantly higher in the case group than in the control group (Figure 2). Forward bowing was a common morphology of the iris in both groups. The height of the anterior bowing reflected the degree of pupillary block. The majority of eyes with primary angle closure (PAC) are caused by the pupillary block mechanism; other non-pupillary block mechanisms, including the plateau iris and forward rotation of the ciliary body may occur

concomitantly.<sup>22</sup> The abnormal position of the lens within the eye can also lead to changes in IF, which explains the higher proportion of type 2, 3, 4, and 5 IFs in the case group.

Wang<sup>6</sup> examined the anatomical structures of the anterior chamber angle using UBM and found that the mechanisms for angle closure in PACG can be categorized into (1) the simple pupillary block mechanism, (2) the simple non-pupillary block mechanism, and (3) the coexistence of multiple mechanisms. The majority of patients with PAC in China have the coexistence of multiple mechanisms. This is consistent with the findings on IC in our study. Figure 5 shows that the IC of the case group is significantly smaller than that of the control group, which indicates the multiplicity of the mechanisms responsible for the occurrence of acute angle closure. Thus, acute angle-closure is the result of the synergy between multiple mechanisms.

The zonules originate from the ciliary processes of the ciliary body and may end at the equator of the lens, the anterior border of the vitreous body, or the pars plana of the ciliary body. Therefore, scholars anatomically categorized them into three types: anterior zonule, posterior vitreous body zonule, and pars plana zonule.<sup>23</sup> Only the anterior zonule is responsible for holding the lens in a relatively stable position within the eyeball; it also plays an important role in adjusting the lens.<sup>24</sup> Our study found that the proportions of cone-like (type 2) and hook-like (type 4) CBCs were significantly higher in the case group than in the control group, but the proportions of parallelogram-like (type 1) and mushroom-like (type 3) CBC were significantly higher in the control group than in the case group (Figure 3). We speculate, in cone-like and hook-like CBCs, the attachment area at the tip of the ciliary process could be smaller; fewer zonules are attached to the ciliary process, and the stability of the lens is poorer. With aging, the lens expands, and its volume and weight also increase. The lens is more likely to move forward or shift from its original position leading to acute angle-closure. Thus, this partly explains the higher proportion of cone-like and hook-like CBCs in the case group. However, in the parallelogram-like and mushroom-like CBCs, the attachment area at the tip of the ciliary process could be larger; more zonules are attached to the ciliary process, leading to higher stability of the lens and a reduced risk of acute angle-closure. Thus, these two types of CBC are more common in the control group. In future studies, we will further explore the relationship between the ciliary body configuration of different types and the position of the lens to verify our conjecture.

Figure 4 shows that the proportions of the BIT types are generally the same in the case and control groups. Both groups had more type 2 and type 3 BITs. The medium-sized pupils and high IOP after the attack did not significantly change the iris thickness. This result is consistent with the findings from the study from Iran conducted by Moghimi.<sup>18</sup> They examined the contralateral eyes of the eyes with acute angle-closure (AAC) and analyzed the quantitative data related to PACS and PACG. They found no significant difference between the iris thicknesses (IT 750  $\mu$ m) of the three groups.

In the case group, the iris was more commonly inserted at the base of the ciliary body, while in the control group, the iris was more commonly inserted in the middle part and the apex of the ciliary body (Figure 6). The case group had more cases of acute angle-closure, while the control group had more cases of open-angle or iridotrabecular contact. Another study by Moghimi<sup>19</sup> also confirmed the above finding. They compared the status of the anterior chamber angles in AAC and contralateral eyes, before and after laser peripheral iridotomy (LPI), and found that the angle opening distance at 500 $\mu$ m from scleral spur (AOD500) of the AAC eyes before LPI was significantly lower than that of the contralateral eyes.

Figure 7 shows that the IA of the case group was significantly smaller than that of the control group. The case group comprised APAC eyes, which may have been complicated by non-pupillary block factors such as forward rotation of the ciliary body. Therefore, the ciliary body was more anterior and closer to the iris, and the angle between the two was smaller. During the attack, the ciliary body was attached to the iris, and the forward rotation pushed the iris up, causing the peripheral iris to move forward and block the anterior chamber angle.

Figure 8 shows that CBS in the case group was significantly smaller than that in the control group. Figure 9 shows that the proportion of the forward rotations of the ciliary body in the case group was significantly higher than that in the control group, and the entire ciliary body was positioned more anteriorly. These are consistent with the findings of Congdon<sup>25</sup> and He.<sup>26</sup> They found that large forward-rotating ciliary processes and plateau irises were associated with the non-pupillary block mechanisms of angle closure. He<sup>26</sup> found that the forward-rotating ciliary processes were more common in operated eyes with persistent angle closure after LPI using the gonioscope in the Liwan eye study. In this study, the position of the ciliary body on the UBM image was marked along its long axis. This method of marking may

accurately indicate the relative position and mechanical direction of the ciliary body in the eyeball.<sup>27,28</sup> However, the studies from Congdon and He determined the values of the relevant parameters based on the direction of the ciliary processes, and this may have caused errors in the data. However, these did not affect the accuracy of the conclusion.

In this study, we had explored and established a new qualitative classification system for angle configurations by UBM. This system could be used to refine and standardize the angle classifications, which also helped to compare and assess the results of various similar studies. Clinically, by dynamically tracking of changes in the qualitative parameters of angle and accurate classifications, it was possible to timely warn the occurrence of APAC and take early intervention when necessary.

In summary, the ciliary body configuration of different types could influence the stability of the lens and the anatomic configuration of the anterior chamber angle indirectly. New qualitative classification system of UBM may be more intuitionistic and refined to reflect the angle configurations to help clinical practice.

## Data Sharing Statement

The data used to support the findings of this study are available from the corresponding author upon request.

## Ethical Approval

The study was approved by the Ethics Committee of The Affiliated Hospital of Qingdao University and conducted in accordance with the principles of the Declaration of Helsinki. Written informed consent was obtained from all subjects.

## Acknowledgments

This work was supported by The Affiliated Hospital of Qingdao University. We would like to express great appreciation to the statistics consultation provided by Professor Zhiying Yu, Penghui Liu and Nan Chen.

## Funding

There were no funding and financially supporting bodies for our research that was not performed as part of the employment of the authors.

## Disclosure

The authors report no conflicts of interest in this work.

## References

- Congdon N, Wang F, Tielsch JM. Issues in the epidemiology and population-based screening of primary angle-closure glaucoma. *Surv Ophthalmol*. 1992;36(6):411–423. doi:10.1016/S0039-6257(05)80022-0
- Rupert RA, Bourne RR, Taylor HR, et al. Number of people blind or visually impaired by glaucoma worldwide and in world regions 1990–2010: a meta-analysis. *PLoS One*. 2016;11(10):e0162229. doi:10.1371/journal.pone.0162229
- Flaxman SR, Bourne RRA, Resnikoff S. Global causes of blindness and distance vision impairment 1990–2020: a systematic review and meta-analysis. *Lancet Glob Health*. 2017;5(12):1221–1234. doi:10.1016/S2214-109X(17)30393-5
- See JL. Imaging of the anterior segment in glaucoma. *Clin Experiment Ophthalmol*. 2009;37(5):506–513. doi:10.1111/j.1442-9071.2009.02081.x
- Prum BE, Herndon LW, Moroi SE, et al. Primary angle closure preferred practice pattern(RR) guidelines. *Ophthalmology*. 2016;123(1):1–40. doi:10.1016/j.ophtha.2015.10.049
- Wang N, Ouyang J, Zhou W, et al. Multiple patterns of angle closure mechanisms in primary angle closure glaucoma in Chinese. *Zhonghua Yan Ke Za Zhi*. 2000;36(1):46–51.
- Lee JR, Sung KR, Han S. Comparison of anterior segment parameters between the acute primary angle closure eye and the fellow eye. *Invest Ophthalmol Vis Sci*. 2014;55:3646–3650. doi:10.1167/iovs.13-13009
- Hata M, Hirose F, Oishi A. Changes in choroidal thickness and optical axial length accompanying intraocular pressure increase. *Jim J Ophthalmol*. 2012;56(6):564–568.
- Dada T, Gadia R, Sharma A. Ultrasound biomicroscopy in glaucoma. *Surv Ophthalmol*. 2011;56(5):433–450. doi:10.1016/j.survophthal.2011.04.004
- He M, Wang D, Jiang Y. Overview of ultrasound biomicroscopy. *J Curr Glaucoma Pract*. 2012;6(1):25–53. doi:10.5005/jp-journals-10008-1105
- Fabijanczyk B, Hagadus R. Role of ultrasound biomicroscopy in the diagnosis and management of glaucoma. *Klin Oczna*. 2005;107(4):316–321.
- Wang FL, Wang DB, Wang L. Characteristic manifestations regarding ultrasound biomicroscopy morphological data in the diagnosis of acute angle closure secondary to lens subluxation. *Biomed Res Int*. 2019;2019. doi:10.1155/2019/7472195.
- Foster PJ, Buhrmann R, Quigley HA, Johnson GJ. The definition and classification of glaucoma in prevalence surveys. *Br J Ophthalmol*. 2002;86(2):238–242. doi:10.1136/bjo.86.2.238

14. Gunning FP, Greve EL. Uncontrolled primary angle closure glaucoma: results of early intercapsular cataract extraction and posterior chamber lens implantation. *Int Ophthalmol*. 1991;15(4):237–247. doi:10.1007/BF00171026
15. Harasymowycz PJ, Papamatheakis DG, Ahmed I. Phacoemulsification and goniosynechialysis in the management of unresponsive primary angle closure. *J Glaucoma*. 2005;14(3):186–189. doi:10.1097/01.jgg.0000159131.38828.85
16. Jiang Y, He M, Huang W, Huang Q, Zhang J, Foster PJ. Qualitative assessment of ultrasound biomicroscopic images using standard photographs: the Liwan eye study. *Invest Ophthalmol Vis Sci*. 2010;51(4):2035–2042. doi:10.1167/iov.09-4145
17. Moghimi S, Vahedian Z, Zandvakil N, et al. Role of lens vault in subtypes of angle closure in Iranian subjects. *Eye*. 2014;28(3):337–343. doi:10.1038/eye.2013.296
18. Moghimi S, Chen R, Hamzeh N, Khatibi N, Lin SC. Qualitative evaluation of anterior segment in angle closure disease using anterior segment optical coherence tomography. *J Curr Ophthalmol*. 2016;28(4):170–175. doi:10.1016/j.joco.2016.06.005
19. Moghimi S, Bijani F, Chen R, et al. Anterior segment dimensions following laser iridotomy in acute primary angle closure and fellow eyes. *Am J Ophthalmol*. 2018;186:59–68. doi:10.1016/j.ajo.2017.11.013
20. Moghimi S, Fathollahzadeh N, Chen R, Lin SC, Weinreb RN. Comparison of fellow eyes of acute primary angle closure and phacomorphic angle closure. *J Glaucoma*. 2019;28(3):194–200. doi:10.1097/IJG.0000000000001167
21. Wang FL, Wang DB, Wang L. Exploring the occurrence mechanisms of acute primary angle closure by comparative analysis of ultrasound biomicroscopic data of the attack and fellow eyes. *Biomed Res Int*. 2020;2020. doi:10.1155/2020/8487907.
22. Nongpiur ME, Ku JY, Aung T. Angle closure glaucoma: a mechanistic review. *Curr Opin Ophthalmol*. 2011;22(2):96–101. doi:10.1097/ICU.0b013e32834372b9
23. Goldberg DB. Computer-animated model of accommodation and theory of reciprocal zonular action. *Clin Ophthalmol*. 2011;5:1559–1566. doi:10.2147/OPTH.S25983
24. Shon K, Sung KR, Kwon J, Hye Jo Y. Vitreous zonule and its relation to anterior chamber angle characteristics in primary angle closure. *J Glaucoma*. 2019;28(12):1048–1053. doi:10.1097/IJG.0000000000001387
25. Congdon NG, Youlin Q, Quigley H, et al. Biometry and primary angle-closure glaucoma among Chinese, white, and black populations. *Ophthalmology*. 1997;104(9):1489–1495. doi:10.1016/S0161-6420(97)30112-2
26. He M, Friedman DS, Ge J, et al. Laser peripheral iridotomy in eyes with narrow drainage angles: ultrasound biomicroscopy outcomes. The Liwan Eye Study. *Ophthalmology*. 2007;114(8):1513–1519. doi:10.1016/j.ophtha.2006.11.032
27. Lee RY, Kasuga T, Cui QN, Huang G, He M, Lin SC. Comparison of anterior segment morphology following prophylactic laser peripheral iridotomy in Caucasian and Chinese eyes. *Clin Experiment Ophthalmol*. 2014;42(5):417–426. doi:10.1111/ceo.12243
28. Huang G, Gonzalez E, Lee R, et al. Anatomic predictors for anterior chamber angle opening after laser peripheral iridotomy in narrow angle eyes. *Curr Eye Res*. 2012;37(7):575–582. doi:10.3109/02713683.2012.655396

## Clinical Interventions in Aging

Dovepress

### Publish your work in this journal

Clinical Interventions in Aging is an international, peer-reviewed journal focusing on evidence-based reports on the value or lack thereof of treatments intended to prevent or delay the onset of maladaptive correlates of aging in human beings. This journal is indexed on PubMed Central, MedLine, CAS, Scopus and the Elsevier Bibliographic databases. The manuscript management system is completely online and includes a very quick and fair peer-review system, which is all easy to use. Visit <http://www.dovepress.com/testimonials.php> to read real quotes from published authors.

Submit your manuscript here: <https://www.dovepress.com/clinical-interventions-in-aging-journal>